Proceedings of the XXIII Conference on Applied Crystallography, Krynica Zdrój, Poland, September 20–24, 2015

The Influence of Technological Parameters of the Casting Process on the Structure and Selected Properties of Iron-Based Metallic Glasses

W. Pilarczyk*, T. Jung and R. Babilas
Silesian University of Technology, Faculty of Mechanical Engineering, Akademicka 2A, Gliwice, Poland

The main aim of this paper was to produce amorphous ribbons with specified composition with the use of various process parameters and X-ray qualitative and quantitative phase analysis after casting and heat treating. Station for ultra-fast cooling of the molten alloy with high vacuum pumps designed for the production of metallic glasses in the form of ribbons with the use of Bühler Melt Spinner SC was used. The X-ray qualitative and quantitative phase analysis, microscopic observation, microhardness and thermal properties tests of the investigated ribbons were conducted. Based on experimental data the discussion on the correlation between casting process parameters, phase and quantitative composition and heat treatment was carried out.

DOI: 10.12693/APhysPolA.130.923
PACS/topics: 61.05.cp, 81.05.Bx, 81.05.Kf, 81.70.Bt, 81.70.Pg

1. Introduction

Multicomponent Fe-based amorphous alloys attract attention due to their good soft magnetic properties combined with high glass-forming ability [1, 2]. These features enable to produce soft ferromagnetic materials in different forms of ribbons, rods, rings or plates. Most often, the soft magnetic properties of metallic glasses can be optimized by applying the appropriate conditions of heat treatment [3–6]. It has been shown that appropriate increase of annealing temperature, significantly improved soft magnetic properties. Therefore, an attempt to correlate casting process parameters, phase and quantitative composition and heat treatment was undertaken.

The Rietveld refinement is the well-known method of structure determination of polycrystalline materials. There are plenty of papers describing the theory and practical aspects of this method, applications of that procedure in structure determination, quantitative phase analysis, crystallite size and lattice strain determination [6, 7].

The presence of Fe–Co–B–Si–Nb amorphous phase in this system has been reported in many research studies [8–11]. The proof for existence of the amorphous, amorphous-crystalline or crystalline component in metallic glasses has been most often obtained from X-ray diffraction (XRD), scanning electron microscopy (SEM), differential scanning calorimetry (DSC) and transmission electron microscopy (TEM) techniques. So far, in its application to phase analysis, XRD has been mostly used as a qualitative tool to identify the products of casting process. No effort has been done until now to quantify the phases — products of casting with the use of different roller rotation speed and heat treatment. The aim of this study has been to produce amorphous ribbons with specified composition and determine the quantitative relations among the products of melt spinning at 10, 20, 30 m/s roller rotation speed and annealing. The Rietveld method in its application to quantitative phase analysis, e.g. PANalytical — High Score Plus software, gives the possibility to follow the changes in both qualitative and quantitative ways.

*corresponding author; e-mail: wirginia.pilarczyk@polsl.pl

2. Experimental procedure

The alloy with a nominal composition of $Fe_{37.44}Co_{34.56}B_{19.2}Si_{4.8}Nb_4$ (at.%) was prepared by induction melting of a mixture of high purity elements (99.9% or higher) in argon atmosphere. Rapidly solidified alloy was prepared by the melt spinning technique (Edmund Bühler Melt Spinner SC) at different linear roller rotation speed. The process parameters are presented in Table I. Figure 1 presents amorphous ribbon made by the use of Bühler Melt Spinner SC station.

TABLE I

Melt spinning process parameters.

roller rotation speed	10, 20, 30 [m/s]
vacuum	7×10^{-2} [mBar]
working pressure	800 [mBar]
casting temperature	1392 [°C]
distance between roller - crucible	0.3 [mm]
injection pressure	400 [mBar]
crucible diameter	20 [mm]

Microstructure observations of the melt-spun ribbons were carried out on the cross-sections of ribbons by means of the Zeiss Supra 35 scanning electron microscope equipped with a chemical composition analysis detector EDS by Oxford.

Fig. 1. Metallic glass in the melt spinner.

Evaluation of qualitative and quantitative phase composition of the obtained materials was made using PANalytical X'Pert PRO diffraction system which uses filtered radiation from the lamp with cobalt anode, with a voltage of 40 kV and heater current of 30 mA. The X-ray phase analysis of the investigated materials was conducted in the Bragg–Brentano geometry using PIXcel 3D detector. Measurements within the 2Θ angle range from 10 to 140° for annealed samples and from 10 to 120° for not annealed samples in steps of 0.026° 2θ were made. A counting time equals 30.6 s per step. The Rietveld quantitative phase analysis was made using PANalytical — HighScore Plus software connected with ICSD database. During the calculation process, the following parameters were optimized: scale factor, flat background, zero shift, lattice parameters, W half width, more background. Quantitative phase analysis has been applied to follow the changes in metallic glasses after casting at different roller rotation speed and annealing.

The study of crystallization process by differential scanning calorimetry method with the use of DSC852 Mettler-Toledo differential scanning calorimeter (Switzerland) was carried out. The sample was analysed in a temperature range of 25–700 °C. The heating rate was 40 °C/min. Analyses were conducted under nitrogen atmosphere (flow of reaction gas 80 mL/min) in open 70 µL alumina crucibles.

Mechanical tests with the use of Future-Tech FM-700_Vickers diamond (hardness) testing machine were carried out.

The amorphous ribbons were annealed at a temperature of 973 K per 1.5 h.

3. Results and discussion

The metallic glasses were obtained with the use of different critical cooling speed. The critical cooling speed was the main parameter which was changing during the ribbons production process. This was done by changing the rotation speed of the roller. The 10, 20, and 30 m/s rotations of the copper roller were used. Dimension of ribbons in as-casted state are presented in Table II.

The thickness of ribbons was found to decrease while the ductility increased with the increase of wheel surface velocity, i.e. with the increase of quenching rate.

TABLE II

Dimension of as-casted ribbons.

ribbon	1 — 10 m/s	2 — 20 m/s	3 — 30 m/s
thickness [μm]	70	60	55
width [mm]	9.2	8.2	7.8

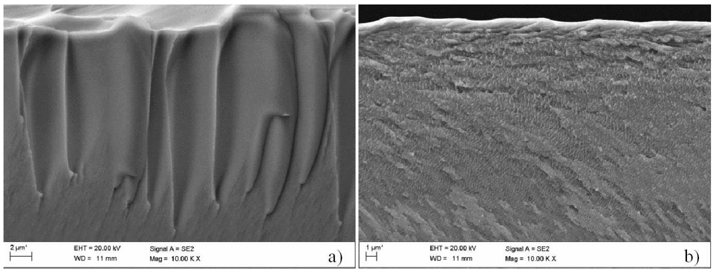

Fig. 2. SEM fracture surface image of Fe–Co–B–Si–Nb ribbons obtained by the use of velocity of roller (a) 10 m/s and (b) 30 m/s, and after decohesion.

The appearance of the fracture surface of the investigated samples in a form of ribbon which were produced with 10 m/s and 30 m/s rotary of copper roller was investigated by SEM and presented in Fig. 2. Every fracture surface appears to consist of two different fracture zones. The fracture could be classified as mixed type with indicated zones containing the river and shell patterns and smooth areas. These patterns are characteristic for metallic glassy alloys.

The presented X-ray diffraction patterns obtained for as-cast state metallic glasses are presented in Fig. 3a. It can be seen that the as-casted $Fe_{37.44}Co_{34.56}B_{19.2}Si_{4.8}Nb_4$ alloy in a form of ribbon was in the amorphous state. The results indicate that the roller rotation speed has no impact on the structure of tested Fe-based alloy at used, precisely determined (Table I) parameters.

The X-ray qualitative phase composition analysis confirmed that the samples before annealing were amorphous but after annealing at a temperature of 973 K during 1.5 h, the following phases appeared: $Fe_{23}B_6$ (ICSD No. 98-005-4786), Fe_2B (ICSD No. 98-004-2530), Fe_3B (ICSD No. 98-061-3889) and Fe_3Si (ICSD No. 98-041-2838) (Fig. 3b–d).

The results of quantitative phase analysis of $Fe_{37.44}Co_{34.56}B_{19.2}Si_{4.8}Nb_4$ ribbons after casting at 10, 20, 30 m/s roller rotation speed and annealing at 973 K are given in Table III.

After crystallisation process at 973 K the phase analysis shows the presence of Fe_3Si, $(Fe,Co)_2B$, $(Fe,Co)_3B$ and $(Fe,Co,Nb)_{23}B_6$ phases. Heat treatment was carried out in temperature higher than sample crystallization temperature (above T_p =880 K and T_p =882 K). However, it should be noted that the presence of residual amorphous halo between 45 and 60°, indicate incomplete crystallization process in all examined materials. Therefore, the percentage of the phases composition

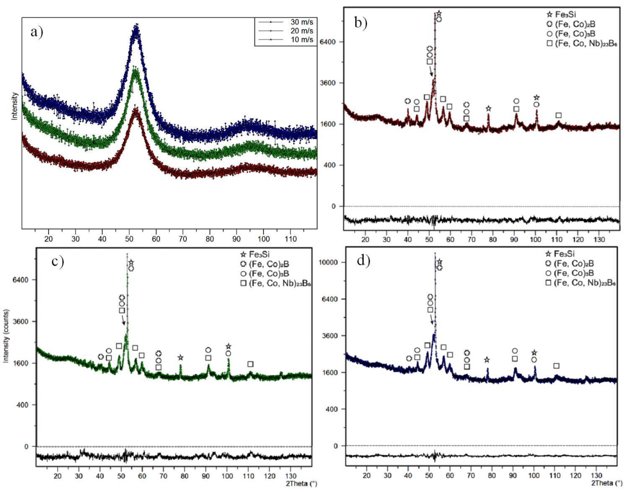

Fig. 3. The X-ray diffraction patterns of the as-casted $Fe_{37.44}Co_{34.56}B_{19.2}Si_{4.8}Nb_4$ alloy in form of ribbons: set of as-casted ribbons (a), as-casted ribbons at 10 m/s (b), 20 m/s (c), 30 m/s (d) roller rotation speed and annealed.

TABLE III

The results of quantitative phase analysis of Fe-based metallic glasses after casting at different roller rotation speed and annealing. Results given in wt%.

phases [wt.%]	1 — 10 m/s	2 — 20 m/s	3 — 30 m/s
Fe_3Si	20.2	23.3	18.0
$(Fe,Co)_2B$	13.3	5.3	6.4
$(Fe,Co)_3B$	13.0	13.4	29.9
$(Fe,Co,Nb)_{23}B_6$	53.5	58.0	45.7

refers solely to the crystalline areas.

The highest fraction of $(Fe,Co,Nb)_{23}B_6$ component, namely 53.5, 58.0, and 45.7 wt% have been obtained in the metallic glasses produced after casting at every roller rotation speed and annealing. Then, the fraction of Fe_3Si phase has a medium content of 20.2 wt% and 23.3 wt% in the sample 1–2 (10, 20 m/s) but it has been reduced to the value of 18.0 wt% in the sample 3 (30 m/s). Thus, there is a considerable rise of content of $(Fe,Co)_3B$ phase to 29.9 wt% (sample 3). $(Fe,Co)_2B$ phase occurs in smaller amount of tested metallic glasses. Mass part totals 13.3, 5.3, and 6.4 wt%, adequately.

Nanocrystallization of complex $Fe_{23}B_6$-type structure in glassy Fe–Co–B–Si–Nb system alloy were studied in [12]. Local structural development in the bulk metallic glass $(Fe_{0.5}Co_{0.5})_{72}B_{20}Si_4Nb_4$ on annealing has been investigated with the use of TEM. In the state prior to the crystallization (below T_g), extended medium range ordered (MRO) regions as small as 2 nm with an extremely high density in the glass matrix were found. Nanoscale crystalline grains with the $Fe_{23}B_6$-type structure were densely formed during annealing around the first crystallization temperature. The nanocrystallized microstructure is presumably ascribed to the presence of the dense MRO regions. The clear $Fe_{23}B_6$ order was found in regions extending as large as 5 nm at a higher temperature (around T_g).

In Table IV research results of thermal properties and microhardness confirming good properties of obtained metallic glasses were put together.

TABLE IV

Results of thermal properties and microhardness of Fe-based ribbons after casting at different roller rotation speed.

ribbon	1 — 10 m/s	2 — 20 m/s	3 — 30 m/s
Hv (cross-section)	1117	1105	1100
Hv (surface)	1115	1102	1095
T_g [K]	822	829	824
T_x [K]	868	871	870
T_p [K]	880	882	882
ΔH [J/g]	57	47	50

The hardness of metallic glass obtained with 10 m/s roller speed of rotation equals 1116 Hv. This is an average hardness value measured on the surface and sample lateral cut, which proves homogeneity of amorphous structure. Sample 1 shows slightly higher hardness value in comparison to other hardness values obtained for samples 2 and 3. This result is comparable with sample sizes (Table II) and occurring stresses due to the brittleness of ribbon number 1.

4. Conclusions

In spite of the fact that the controlling of the nanocrystallisation process seems to be also the controlling of material properties, the structure studies such as the quantity phase analysis, the finding of the crystallisation temperature, chosen properties tests, and process production parameters are important aspects of searching materials.

In this paper, the results of the X-ray studies on the Fe–Co–B–Si–Nb alloy structure with the use of using the Rietveld method, microscopic observation, thermal and hardness tests were presented.

Right after casting the ribbon characterises with the amorphous structure. The hardness measuring showed that conventional metallic glasses of $Fe_{37.44}Co_{34.56}B_{19.2}Si_{4.8}Nb_4$ chemical composition reach hardness values above 1100 Hv. Hardness measured on the surface and lateral cut reaches similar values which can prove homogeneous structure.

Thermal analysis proved good vitrification ability of metallic glasses which were obtained with the use of different casting process parameters. Characteristic temperatures T_g, T_x, T_p reach values of the same temperature range. Simultaneously DSC research allowed to choose thermal treatment parameters.

Dominant ingredient in metallic glasses right after casting regardless the used casting process conditions and also after annealing is $(Fe,Co,Nb)_{23}B_6$ phase. Fe_3Si phase creates the second in respect of mass participation ingredient of every tested sample. The smallest ratio is ascribed to $(Fe,Co)_2B$ phase.

The critical cooling speed is dependent on the roller rotation speed. On the basis of the investigation, it was concluded that the critical cooling speed does not significantly affect the thermal properties and hardness of the ribbons using the chosen, determined parameters of roller rotation speed. It can be noticed that critical cooling speed has no impact on the results of quantitative phase analysis of Fe-based metallic glasses after casting at different roller rotation speed and annealing.

Acknowledgments

The work was supported by National Science Centre under research project no. 2011/03/D/ST8/04138.

References

[1] R. Piccin, P. Tiberto, M. Baricco, *J. Alloys Comp.* **434-435**, 628 (2007).

[2] X.M. Huang, X.D. Wang, J.Z. Jiang, *J. Alloys Comp.* **485**, 35 (2009).

[3] D. Li, Z. Lu, S. Zhou, *Sensor. Actuat. A Phys.* **109**, 68 (2003).

[4] N.Q. Hoa, D.T.H. Gam, N. Chau, N.D. The, S.C. Yu, *J. Magn. Magn. Mater.* **310**, 2483 (2007).

[5] S.S. Yoon, N.A. Buznikov, L. Jin, C.O. Kim, C. Kim, *J. Magn. Magn. Mater.* **304**, 186 (2006).

[6] M. Karolus, *J. Mater. Proc. Tech.* **175**, 246 (2006).

[7] V. Recarte, J.I. Perez-Landazabal, C. Gomez-Polo, *Physica B* **350**, 135 (2004).

[8] A. Inoue, B.L. Shen, C.T. Chang, *Acta Mater.* **52**, 4093 (2004).

[9] W. Pilarczyk, *J. Achiev. Mater. Manufact. Eng.* **52**, 83 (2012).

[10] W. Pilarczyk, A. Pilarczyk, *Mater. Technol.* **49**, 537 (2015).

[11] A. Urata, N. Nishiyama, K. Amiya, A. Inoue, *Mater. Sci. Eng. A Struct.* **449-451**, 269 (2007).

[12] A. Hirata, Y. Hirotsu, K. Amiya, N. Nishiyama, A. Inoue, *Intermetallics* **16**, 491 (2008).